Vesicle Membrane Interactions of Penetratin Analogues†

Daniel Persson,* Per E. G. Thorén, Per Lincoln, and Bengt Nordén

Department of Chemistry and Bioscience, Chalmers University of Technology, SE-412 96 Gothenburg, Sweden

Received November 17, 2003; Revised Manuscript Received June 17, 2004

ABSTRACT: Reports on serious artifacts associated with the use of cell fixation in studies of the cellular uptake of cell-penetrating peptides, also denoted protein transduction domains, have demonstrated the need for a reevaluation of the current understanding of peptide-mediated cellular delivery of large, hydrophilic molecules. In a recent study on the internalization in unfixed cells of penetratin and its analogues in which tryptophans are substituted for phenylalanines (Pen2W2F), lysines for arginines (PenArg), and arginines for lysines (PenLys), we revealed large dissimilarities in cell interactions among the peptides [Thorén et al. (2003) *Biochem. Biophys. Res. Commun. 307*, 100−107]. We here investigated possible correlations with their respective affinities for the lipid membranes of large unilamellar vesicles. The variations found in membrane affinity correlated qualitatively with differences in hydrophobicity among the peptides but were by far too small to account for the striking differences in cell membrane binding. Interestingly, we found that the inclusion of a small fraction of lipids conjugated to poly(ethylene glycol) (PEG) in the vesicles both stabilized the vesicle dispersion against peptide-induced aggregation and, furthermore, enhanced the binding of the peptides to the membrane. By use of PEG-conjugated lipids, it could be shown that vesicle aggregation drives an α-helix to β-sheet conformational transition for these peptides. A similar transition was discovered at submicellar concentrations of sodium dodecyl sulfate in aqueous solution for all peptides except PenLys. Finally, significant changes of the contributions to CD spectra from aromatic residues due to their insertion into the membrane were observed.

Intracellular delivery of large, hydrophilic molecules, such as oligonucleotides and proteins, is hampered by their poor plasma membrane permeability. However, with the identification of a number of cell-penetrating peptides (CPPs)[1] that are able to transport large cargos into cells, this obstacle now seems surmountable (*1, 2*). One of the most widely studied CPPs is penetratin, a 16-mer peptide derived from the homeodomain of the *Drosophila* transcription factor Antennapedia (*3*). Until recently, studies of the cellular uptake of penetratin have almost exclusively been based on fluorescence microscopy on fixed cells (*3*−*5*). In studies on fixed cells, internalization of penetratin was basically unaltered by modifications such as reversal of the amino acid sequence, substitution of all amino acids for their D-enantiomers or introduction of three helix-breaking proline residues. However, substitution of its two tryptophans was reported to virtually abolish the ability to translocate across the plasma membrane. Taken together with observations of efficient internalization also at low temperature, when active, ATP-driven transport should not operate, this lead to a common view of an energy- and receptor-independent, nonendocytotic uptake, where peptide conformation is of minor importance but with the two tryptophans in the peptide sequence playing key roles in an, as yet, unknown translocation mechanism. Studies of the cellular uptake of arginine-rich peptides suggested that also the arginines could be important (*6*, *7*). All these findings will now, however, have to be reevaluated, because two studies have unequivocally demonstrated that crucial artifacts may arise as a result of cell fixation in studies of cellular uptake of CPPs (*8*, *9*). It was shown that fixation causes artifactual uptake of peptide bound to the cell surface, leading to misinterpretations since these often cationic peptides have a strong affinity for the plasma membrane and are not removed even by repeated washings. Also, it was found that peptide internalized by endocytosis may be redistributed during fixation.

These discoveries demonstrated the urgent need for new cell internalization studies. In a recent paper (*10*), therefore, we assessed the cellular uptake of a number of penetratin analogues in live, unfixed cells (rat adrenal pheochromocytoma cells (PC-12) and Chinese hamster lung fibroblasts (V79)). Indeed, in contrast to previous findings from studies on fixed cells, we found that penetratin was taken up via endocytosis, as was the analogue Pen2W2F, in which the

† Supported by the Strategic Nucleic Acid Research Program and the Swedish Research Council.

* Corresponding author. Fax: (46)-31-7723858. E-mail: danielp@phc.chalmers.se.

[1] Abbreviations: ATP, adenosine triphosphate; CD, circular dichroism; CPP, cell-penetrating peptide; DOPC, 1,2-dioleoyl-*sn*-glycero-3-phosphocholine; DOPG, 1,2-dioleyol-*sn*-glycero-3-phosphoglycerol; DPPC, 1,2-dipalmitoyl-*sn*-glycero-3-phosphocholine; DPPS, 1,2-dipalmitoyl-*sn*-glycero-3-phosphoserine; DSPE-PEG(2000), 1,2-distearoyl-*sn*-glycero-3-phosphoethanolamine-*N*-[poly(ethylene glycol)2000]; EDTA, ethylenediaminetetraacetic acid; HEPES, *N*-(2-hydroxyethyl)-piperazine-*N*′-(2-ethanesulfonic acid); HPLC, high-performance liquid chromatography; LUVs, large unilamellar vesicles; OD, optical density; PEG, poly(ethylene glycol); PEI, poly(ethylenimine); PM-IRRAS, polarization modulation infrared reflection absorption spectroscopy; POPC, 1-palmitoyl-2-oleoyl-*sn*-glycero-3-phosphocholine; POPG, 1-palmitoyl-2-oleoyl-*sn*-glycero-3-phosphoglycerol; SDS, sodium dodecyl sulfate; SUVs, small unilamellar vesicles; SVD, singular value decomposition; TFE, 2,2,2-trifluoroethanol; UV, ultraviolet.

10.1021/bi036054d CCC: $27.50
Published on Web 07/29/2004

two tryptophans were substituted for phenylalanines. By contrast, for PenArg, an analogue in which the lysines of penetratin were replaced with arginines, the endocytotic uptake was also paralleled by internalization via an apparently ATP-independent, nonendocytotic pathway. Surprisingly, the penetratin analogue in which the arginines were substituted for lysines (PenLys) exhibited no cellular uptake at all and a very low affinity for the plasma membrane. It should be noted that even though these results indicate an endocytotic uptake of penetratin, there are a large number of studies in which various membrane-impermeable molecules, when conjugated to penetratin, have been shown to have the desired biological activity (see refs *11* and *12* for a review). This implies that the conjugates must, to some extent, be able to escape the endosomes without extensive degradation. An indication of this was found in the observation that small amounts of peptide reached the nucleus in a substantial fraction of the cells (*10*).

In this study, we apply a recently developed method of analysis (*13*) to measure the binding of penetratin and its analogues PenArg and PenLys to negatively charged vesicles, in search of clues to the observed vast differences between the peptides in cell association. Due to a strong propensity of PenArg to aggregate vesicles, the binding of this peptide to DOPC/DOPG liposomes was difficult to assess. Therefore, we also determined the binding isotherms for association to vesicles stabilized by PEG-conjugated lipids. Furthermore, we assessed the conformational states of all four peptides in their interactions with vesicle membranes using circular dichroism spectroscopy, and we also extended a previously published study in which we observed that penetratin at high peptide-to-lipid ratios induces vesicle aggregation followed by spontaneous disaggregation in a process that involves simultaneous conformational changes of the peptide (*14*).

MATERIALS AND METHODS

Materials. 1,2-Dioleoyl-*sn*-glycero-3-phosphocholine (DOPC) was purchased from Larodan. 1,2-Dioleoyl-*sn*-glycero-3-phosphoglycerol (DOPG), 2,2,2-trifluoroethanol (TFE), and polyethylenimine (50% (w/v) aqueous solution) were obtained from Sigma. 1,2-Distearoyl-*sn*-glycero-3-phosphoethanolamine-*N*-[poly(ethylene glycol)2000] (DSPE-PEG(2000)) was purchased from BioTrend. 5-(and 6-)Carboxyfluorescein was obtained from Molecular Probes.

For circular dichroism measurements, a 1 mM sodium phosphate buffer (pH 7.4) was employed. For the induced leakage assay, the buffer used was 10 mM HEPES, 5 mM NaOH, 1 mM EDTA, and 107 mM NaCl (pH 7.4). The buffer used in all other experiments was 10 mM HEPES, 5 mM NaOH, 1 mM EDTA, and 0.1 M NaCl (pH 7.4). Deionized water from a Milli-Q system (Millipore) was used.

Peptide Synthesis. Penetratin (RQIKIWFQNRRMKWKK), PenArg (RQIRIWFQNRRMRWRR), PenLys (KQIKIWFQNKKMKWKK), and Pen2W2F (RQIKIFFQNRRMKFKK) were synthesized as described previously with acetylated amino termini and amidated carboxyl termini (*15*).

Vesicle Preparation. Chloroform solutions of DOPC, DOPG, and for some experiments also DSPE-PEG(2000) were mixed, and the solvent was removed with a rotary evaporator. The dry phospholipid film was placed in high vacuum (~0.1 Torr) for 2 h to remove trace amounts of chloroform. Vesicles for binding studies and circular dichroism measurements were prepared by dispersion of the lipid film in buffer. Vesicles with encapsulated carboxyfluorescein for leakage experiments were prepared by dispersion of the lipid film in a 10 mM HEPES, 50 mM carboxyfluorescein, 10 mM NaCl, 148 mM NaOH, and 1 mM EDTA (pH 7.4) solution. The dispersion was subjected to five freeze−thaw cycles (*16*) before extrusion 21 times through two 100 nm polycarbonate filters on a LiposoFast pneumatic extruder (Avestin, Canada) to obtain large unilamellar vesicles (LUVs). The lipid concentration was determined by the Stewart assay (*17*). A homogeneous liposome size distribution around 100 nm was confirmed by dynamic light scattering analysis using a Malvern Instrument series 7032 Multi-8 correlator and a PCS100 spectrometer (Malvern Instruments).

Peptide Concentrations. The concentrations of penetratin, PenArg, and PenLys, each containing two tryptophans, were determined from the UV absorbance measured on a Cary 4B UV−vis spectrometer using an ϵ_{280} for tryptophan of 5690 M^{-1} cm^{-1} (*18*). Pen2W2F concentrations were established by measuring the absorption spectra of water solutions of this peptide and of 2 mM free phenylalanine between 230 and 340 nm. The latter spectrum was then scaled in small steps, and the resulting spectra were subtracted from the peptide spectrum. By visual inspection of the difference spectra, the scale factor that leads to elimination of the peak at 257.5 nm was determined, and thereby the concentration of Pen2W2F could be calculated. The absorbance measurements showed that the concentrations of all peptides were only around 70% of the nominal concentrations from weighing in of the freeze-dried peptides. This explains a discrepancy between the CD spectra for penetratin presented here and those reported earlier (*13*, *14*). Together with a difference in lipid concentration, based on the assumption that only lipids in the outer leaflet are accessible for the peptides, it contributes to the marked differences that may be noted between the binding isotherms for penetratin presented here and those reported previously for the same peptide (*13*).

Binding Experiments. Fluorescence experiments were performed on a Spex Fluorolog τ-3 spectrofluorometer (JY Horiba) using a 1 cm × 1 cm quartz cell thermostated at 25 °C. The band-pass of the excitation slit was set to 0.7 nm to obtain an optimal signal-to-noise ratio without photodegradation. Spectra were recorded between 315 and 400 nm with an increment of 1 nm and an integration time of 2 s. The total concentration of peptide in the samples was ~2 μM. Peptide solution was titrated with microliter aliquots of liposome stock solution (5 mM), and a spectrum was acquired after every vesicle addition. Above certain peptide-to-lipid ratios, the peptides studied here induce vesicle aggregation. The presence of large aggregates is expected to influence the absorption as well as the fluorescence of the sample, thereby distorting the apparent binding isotherms. Therefore, the samples were checked for aggregation by static light scattering with both the excitation and the emission monochromators set to 600 nm. Mixing of the cuvette contents was achieved by plunging a cuvette mixer three times up and down. It was shown in separate experiments using various fluorophores that this procedure was sufficient for complete mixing. The cuvette mixer was constructed in

stainless steel with a straight handle and a rhombic footprint with diagonals of 13 and 10 mm.

To minimize peptide adsorption, the surface of the interior cuvette walls was modified by leaving the cuvette filled with a 1% (w/v) solution of polyethylenimine in deionized water at room temperature for 30 min. The cell was then rinsed thoroughly with deionized water.

Analysis of Binding Data. Spectra were corrected by subtracting the vesicle background, measured in a separate experiment, and analyzed using Matlab (The MathWorks Inc.). For singular value decomposition of the titration spectra (eq A1, see Appendix), the Matlab command *svd* was employed, and for least-squares projection of titration spectra on reference spectra (eq A3), the *pinv* command was used.

Circular Dichroism Measurements. Circular dichroism (CD) was measured on a Jasco J-810 spectropolarimeter at 25 °C using a 1 mm quartz cell for peptide concentrations of ~7 μM and a 10 mm quartz cell for peptide concentrations of 0.5−1.5 μM. All spectra were taken between 190 and 260 nm and corrected for background contributions. Results are expressed as mean residue ellipticities, $[\theta]_{MR}$ (deg cm^2/dmol). The fraction of α-helix conformation in the peptides was estimated from the mean residue ellipticities at 222 nm using the equation $[\alpha] = [\theta]_{222}/(-39\,500(1 - k/n))$, where $[\alpha]$ is the fraction of α-helix, k is a wavelength-dependent factor equal to 2.57 at 222 nm, and n is the number of amino acids in the peptide (*19*). Due to extensive absorption of light in the far-UV by polyethylenimine, CD cuvettes were not surface-modified.

Monitoring Vesicle Aggregation and Dissociation. Aggregation and dissociation of liposomes could be continuously monitored from changes in turbidity. Measurements of optical density (OD) were performed on either a Cary 4B UV−vis spectrometer or a Jasco V-530 UV−vis spectrometer at 436 nm or at 250 nm. All measurements were carried out at room temperature in a 1 cm quartz cell with a sample volume of 3 mL.

Induced Leakage Assay. The efflux experiments were performed at 25 °C on a Spex Fluorolog τ-3 spectrofluorometer (JY Horiba). The nonentrapped dye was separated from the vesicles on a Sephadex G-50 column (Amersham Pharmacia Biotech) by using an isoosmolar buffer (see above). Lipid concentrations were determined by static light scattering at 600 nm using a standard curve. Peptide-induced leakage of vesicle-entrapped carboxyfluorescein was monitored using excitation and emission wavelengths of 490 and 520 nm, respectively. The liposomes were diluted with buffer in a 1 cm × 1 cm quartz cell before addition of peptide. Starting with a self-quenching concentration of carboxyfluorescein inside the liposomes, any leakage of the dye can be detected as an increase in the fluorescence intensity. The peptide-induced leakage can be quantified by relating it to the effect of lysing the vesicles with Triton X-100. The self-leakage of the dye was found to be negligible and was not affected by the polyethylenimine modification of the cuvette walls.

RESULTS AND DISCUSSION

Binding Isotherms. The binding of penetratin and its analogues in which the lysines were substituted for arginines (PenArg) or vice versa (PenLys) to LUVs was studied using the blue shift of the tryptophan fluorescence emission maximum and the concomitant increase in fluorescence quantum yield as the peptides associate with lipid membranes. A peptide solution was titrated with small volumes of liposome stock solution, and tryptophan emission spectra were acquired after every addition. The spectra were analyzed by a method proposed by Polozov et al. (*20*), and further developed in previous work on the membrane binding of penetratin (*13*). By projecting the titration spectra on reference spectra of free and membrane-bound peptide, we could determine the concentrations of these two species at various defined lipid concentrations , allowing direct construction of binding isotherms. This method is preferable especially when studying vesicle association of peptides prone to adsorb to surfaces, as was the case here. For a description of the surface adsorption characteristics of penetratin, to which those of PenArg and PenLys were found to be similar, see refs *13* and *21*. Since reference spectra can be recorded in separate experiments where the sample is mixed only once, minimizing peptide adsorption, and the actual peptide concentration in the very same sample can be determined by measuring the tryptophan absorption, the emission spectra of defined concentrations of free and membrane-bound peptide are obtained with high accuracy. The variation of the total peptide concentration in the titration due to adsorption to the cuvette walls, the pipet tips, and the mixing device is thus not a problem and can even be followed quantitatively during the experiment.

In this work, we characterized the interaction of penetratin and its analogues, PenArg and PenLys, to DOPC/DOPG (molar ratio 60/40) as well as DOPC/DOPG/DSPE-PEG-(2000) (molar ratios 60/37.5/2.5) LUVs. For all titrations, it was found by singular value decomposition (SVD) of the titration spectra that two species, free and membrane-bound peptide, account for the spectral data (data not shown). The least-squares projection analysis thus gives the concentrations (C_f and C_b) of these two species (see Appendix). With C_f and C_b determined for every lipid concentration, L, in the titration, the membrane-bound peptide to lipid molar ratio,

$$r = \frac{C_b}{L} \tag{1}$$

can be calculated and the binding isotherm, r versus C_f, constructed. It should be noted that when r was calculated, the peptides were assumed to stay in the outer leaflet, since it was shown in other experiments that although they all easily traverse the membranes of giant unilamellar vesicles, none of the peptides can translocate across the bilayers of DOPC/DOPG LUVs (unpublished experiments). Furthermore, the proportion of the total amount of lipid residing in the outer leaflets of the vesicles was taken as the theoretical value 54%, calculated for a sphere with a diameter of 100 nm and a bilayer thickness of 4 nm. Figure 1A shows the binding isotherms for all three peptides in the two types of liposomes studied. The marked curvature stems from the decreased electrostatic attraction between the peptide and the membrane as more and more peptide is associated with the vesicles (*22*, *23*) and can be accounted for by Gouy−Chapman theory (see below). For every peptide, the first vesicle addition in the DOPC/DOPG titrations was adjusted to be just large enough to avoid aggregation and as is obvious

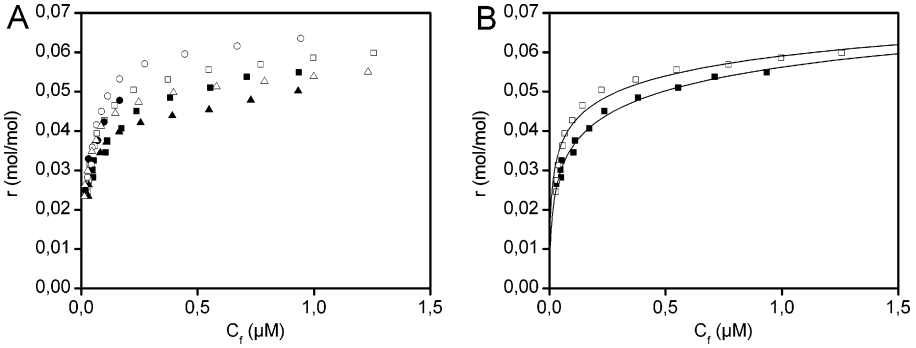

FIGURE 1: Panel A presents binding isotherms for the association of penetratin (squares), PenArg (circles), and PenLys (triangles) to DOPC/DOPG (molar ratio 60/40, filled symbols) and DOPC/DOPG/DSPE-PEG(2000) (60/37.5/2.5, open symbols) vesicles. The membrane-bound peptide to lipid molar ratio, r, is plotted against the free peptide concentration in bulk solution, C_f. Panel B presents experimental binding isotherms for penetratin (squares) and theoretical binding isotherms (solid lines) calculated according to a model combining Gouy−Chapman theory with a surface partition equilibrium (see Appendix for details). Values of the effective peptide charge, z_p, and the surface partition constant, K_p, are given in Table 1.

from Figure 1A, it was impossible to obtain a complete binding isotherm for PenArg association to the PEG-free vesicles. The stronger tendency of PenArg to cause vesicle aggregation is somewhat surprising. However, due to its higher membrane affinity, the bound peptide-to-lipid ratio at which aggregation occurs for PenArg is not very far from those observed for penetratin and PenLys despite the considerably lower total peptide concentration.

For liposomes containing PEG−lipid conjugates, the grafted PEG moieties are thought to act as steric barriers, hindering bilayer−bilayer contact (*24*−*27*). In the vesicle system used here, the inclusion of 2.5 mol % PEG-conjugated lipids in the membranes had a remarkable effect on the stability of the liposome dispersion, radically extending the range of applicable total peptide-to-lipid ratios for all three peptides. For PenArg, minor aggregation with PEG-modified liposomes was observed at peptide concentrations above that corresponding to the last point in the binding isotherm in Figure 1A, whereas for penetratin and PenLys, no aggregation in this system was obtained even at extreme total peptide-to-lipid ratios (data not shown). From the binding isotherms, it is obvious that PenLys has a slightly lower affinity than penetratin for both types of vesicle membranes. Penetratin, in turn, has a slightly lower membrane affinity than PenArg. Also noteworthy is that the peptides have a higher affinity for the PEG-modified vesicles than for the PEG-free ones. Fitting of the experimentally determined binding isotherms to a binding model that has previously been found to describe well the binding of penetratin to DOPC/DOPG liposomes with a DOPG content ranging from 10% to 40% (*13*), provides more information on the membrane association of the peptides.

The binding model used here for comparison of the binding isotherms is based on the Gouy−Chapman theory in combination with a two-state partition equilibrium (see Appendix). In the fitting of the model to data, the values of two parameters are obtained: the effective charge of the peptide, z_p, and the surface partition constant, K_p. For the DOPC/DOPG liposomes, the calculated binding isotherms are in good agreement with the experimental data (Figure 1B). The resulting optimal values of z_p and the corresponding values of K_p are presented in Table 1. In the case of PenArg, though, only a few data points at low C_f values were obtainable in the titrations, and accordingly, the parameters

Table 1: Summary of Binding Parameters

DOPC/DOPG (molar ratio 60/40)	K_p (M^{-1})[a]	z_p[b]	ΔG_h (kcal/mol)[c]
PenLys	404 ± 50[d]	4.3 ± 0.4[d]	−3.55 ± 0.07[d]
penetratin	534 ± 54	3.9 ± 0.2	−3.72 ± 0.05
PenArg	1472 ± 504[e]	3.5 ± 0.3[e]	−4.32 ± 0.17[e]
DOPC/DOPG/ DSPE-PEG(2000) (molar ratios 60/37.5/2.5)	**K_p (M^{-1})[a]**	**z_p[b]**	**ΔG_h (kcal/mol)[c]**
PenLys	579 ± 43	4.7 ± 0.3	−3.77 ± 0.05
penetratin	907 ± 61	4.3 ± 0.3	−4.03 ± 0.04
PenArg	1891 ± 221	4.2 ± 0.3	−4.47 ± 0.08

[a] Surface partition constant. [b] Effective peptide charge. [c] Hydrophobic contribution to ΔG ($-RT \ln K_p$, see eq 2). [d] The errors define the limits of the interval within which the sum of square errors is less than twice that of the best fit. [e] Calculated from insufficient data.

calculated should be considered uncertain. It is noteworthy that for reasons outlined in Materials and Methods, the partition constant for penetratin association to DOPC/DOPG liposomes differs significantly from that presented earlier (*13*). For all three peptides, in both sets of vesicles, the calculated z_p values are smaller than the formal charge, which is +7 (both the carboxyl termini and the amino termini are end-capped). This observation has been made in studies of a number of charged peptides and has been attributed mainly to discrete charge effects (see refs *28* and *29* and references therein), separation of charges in the peptide (*22*, *30*), and effects of associated counterions (*28*).

Influence of Inclusion of PEG-Conjugated Lipids on Peptide Binding. Whereas the applied binding model, which is based on Gouy−Chapman theory in combination with a simple two-state partition equilibrium, describes well the binding isotherms for peptide association to DOPC/DOPG liposomes, small deviations were obtained (see Figure 1B) when trying to fit it to the isotherms for peptide association to liposomes containing PEG-conjugated lipids. This suggests that in these systems, additional interactions need to be considered. Somewhat surprisingly, these PEG-related interactions are apparently attractive in nature, judging from the binding isotherms and the binding parameters obtained when trying to fit the binding model to them (Table 1). There are a great number of reports on how inclusion of PEG-conjugated lipids in liposomes has significantly reduced or

even abolished protein adsorption on liposomes (see *31* and *32* and references therein). This effect has often been ascribed to steric repulsion of the large protein molecules, but a potential influence of the PEG moieties on the hydration of the membrane surface has also been proposed. For smaller molecules, such as oligopeptides, the steric repulsion might be negligible, and indeed, the presence of PEG-conjugated PE in PC LUVs has been shown to increase the membrane affinity of melittin and the presequence of the mitochondrial peptide rhodanese (MPR) (*33*, *34*). Although it is claimed that the promoted peptide association is due to the electrostatic attraction resulting from the inclusion of negatively charged PEG-PE conjugates to the lipid mixture, it is not clear-cut that the effect can be entirely ascribed to electrostatics. In an extensive review, Vermette and Meagher (*32*) discuss many types of interactions that might be important in peptide/protein association to PEG-modified liposomes, including hydrogen bonding, hydrophobic interactions, and van der Waals attraction. However, in the present study of penetratin peptides, we could not prove any direct interactions with the PEG moieties, since SVD analysis of the fluorescence emission spectra gave no indication of a third species in the PEG-containing liposomes and the spectra for completely bound peptides were identical in the two types of vesicles. Also, CD studies reveal no significant differences between the conformations of peptides associated with PEG-free or PEG-modified vesicles (see below). Possibly, the increased membrane affinity is related, directly or indirectly, to a destabilization of the vesicular bilayer induced by the PEG-conjugated lipids. Such an effect has been observed in a number of studies, manifested by increased membrane permeability to glucose and calcein (*35*−*37*). Certainly, destabilization of the lipid bilayer per se could promote peptide partitioning into the membrane. Alternatively, albeit less likely, peptide translocation might be made possible by PEG destabilization of the membrane, rendering also the inner leaflets accessible to the peptide.

Whatever the origin of the apparently higher affinity for the PEG-containing membranes, the effect amounts to 0.2−0.3 kcal/mol as judged from the changes in hydrophobic free energy for penetratin and PenLys (see Table 1). When applied to PenArg, this would indicate a ΔG_h somewhere between −4.1 and −4.3 kcal/mol for association to DOPC/DOPG LUVs.

Free Energy of Binding. Penetratin and its analogues exhibit surface partition constants in the range between the moderately hydrophobic peptide magainin 2 amide (K_p = 50 M^{-1}) (*38*) and melittin ($K_p = 4.5 \times 10^4$ M^{-1}) (*39*), which has a high content of nonpolar amino acids. The total free energy of binding can be calculated as

$$\Delta G = -RT\left[\ln 55.5 + \ln K_p + \ln\left(\frac{C_M}{C_f}\right)\right] \qquad (2)$$

where the first term provides the cratic contribution (*40*), equal to −2.4 kcal/mol, the second term represents the hydrophobic contribution (*23*, *41*), and the term $\ln(C_M/C_f)$ represents the electrostatic contribution to the binding energy. For all three peptides, the hydrophobic and the electrostatic contributions to the total free energy of binding are of the same order of magnitude. In the case of, for example, penetratin binding to the PEG-free vesicles, the electrostatic free energy contribution is found to be −5.51 kcal/mol at low degrees of binding, compared to the value −3.72 kcal/mol for the hydrophobic contribution. The main driving force for the partitioning of peptide into the membrane is the so-called hydrophobic effect (the total free energy gain by removing nonpolar parts of a peptide from the aqueous phase) (*42*) and the formation of inter- or intramolecular hydrogen bonds as the peptide forms a secondary structure (*43*). Free energy calculations, based on the whole-residue hydrophobicity scale of Wimley and White (*44*) and the helicities of the peptides as estimated from circular dichroism measurements (see below), were carried out along the lines of our previous work (*13*). These calculations largely reproduced the differences in the experimental hydrophobic free energies between peptides (data not shown).

Correlation with Binding to Cellular Membranes. There are obvious differences among the peptides in their affinity for the types of membranes studied here, but they are definitely not of such a magnitude that they could explain the large differences in cell association observed in our recent experiments on the uptake of these peptides in live cells (*10*). In that study, incubation of PC-12 and V79 cells with PenArg and penetratin resulted in rapid and extensive peptide binding, mostly in patches, to the plasma membranes, whereas PenLys exhibited only very sparse membrane association. Upon cell association, PenArg and penetratin were internalized, apparently mostly by endocytosis, but at least PenArg was also taken up via another, nonendocytotic, pathway. In light of the results on peptide binding to vesicles obtained here, it is probable that in their interaction with plasma membranes, PenArg and penetratin bind specifically to certain lipids present there, or even more likely, to other components at the extracellular surface, such as polysialic acid or heparan sulfate proteoglycans. Indeed, the guanidinium group of arginine can form strong bidentate hydrogen bonds with anions such as phosphate, carboxylate, and sulfate (for a review, see ref *45*). However, as we shall see, conformational studies provide an alternative explanation to the dissimilarities in cell association.

Peptide Conformation. Whereas PenArg and PenLys have not been studied previously, penetratin and Pen2W2F have been the subject of a number of conformational studies in various membrane-mimicking environments. In aqueous solutions, the conformation of penetratin has been found to be largely random coil (*46*−*48*), whereas in SDS micelles (*46*, *47*, *49*), as well as in trifluoroethanol (*48*), the peptide has spectra characteristic of an α-helix. In liposomes, the secondary structure of penetratin is dependent on the experimental conditions. Thus, we have earlier reported that at low peptide-to-lipid ratios, penetratin adopts an α-helical conformation that is independent of surface charge density when bound to DOPC/DOPG or pure DOPG LUVs (*13*, *14*). α-Helix formation of penetratin has also been observed at low peptide-to-lipid ratios for POPC/POPG (70/30) SUVs (*47*, *50*) and POPG SUVs (*50*). On the other hand, at higher membrane concentrations of peptide, we have observed formation of antiparallel β-pleated sheets in DOPG LUVs (*14*). Interestingly, it was found that there exists a certain peptide-to-lipid ratio above which penetratin induces vesicle aggregation followed by spontaneous disaggregation. Strongly coupled to this process was a conformational transition of the peptide from α-helix to β-sheet during aggregation and

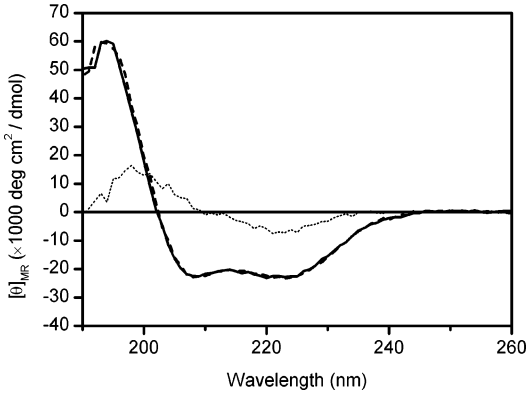

FIGURE 2: Circular dichroism spectra of penetratin bound to DOPC/DOPG (60/40, solid line) and DOPC/DOPG/DSPE-PEG(2000) (60/37.5/2.5, dashed line) liposomes. The peptide concentration was 7 μM, and the concentration of lipid was 500 μM. The difference spectrum (dotted line) between penetratin (7 μM) associated with DOPC/DOPG (60/40, 500μM) and penetratin (7 μM) in trifluoroethanol/water (9/1) is also included.

then back to an α-helical conformation during disaggregation of the vesicles. The same phenomenon was observed in the present study for DOPC/DOPG (60/40) vesicles but not for liposomes containing PEG-PE (see below). Magzoub et al. has reported a similar conformational transition for penetratin at elevated peptide-to-lipid ratios in POPC/POPG (70/30) and pure POPG SUVs (*50*). However, they did not report any observations of vesicle aggregation, which is surprising considering the strong coupling of the processes as has been observed in our laboratory. Formation of antiparallel β-sheets has also been observed in DPPC/DPPS monolayers using PM-IRRAS (*51*). The doubly phenylalanine-substituted penetratin peptide, Pen2W2F, has been found to adopt a random coil conformation in aqueous solution (*48*, *52*) and to form an α-helix in TFE (*48*). In POPC/POPG (70/30) SUVs, both α-helix and β-structures were reported (*52*).

The circular dichroism spectra of penetratin in nonaggregated DOPC/DOPG (60/40) and DOPC/DOPG/DSPE-PEG-(2000) (60/37.5/2.5) LUVs were, within experimental errors, found to be superimposable (Figure 2). The same observation was made for PenArg, PenLys, and Pen2W2F. PenArg and PenLys gave rise to CD spectra very similar in shape to that of penetratin, but with a slightly lower magnitude overall for PenArg and a slightly higher one for PenLys (data not shown). For the three tryptophan-containing peptides, there is clearly a substantial α-helical content, and helicities of 61%, 67%, and 74% for PenArg, penetratin, and PenLys, respectively, were estimated from the molar residue circular dichroism at 222 nm (see Materials and Methods). The spectrum of Pen2W2F (see Figure 5), on the other hand, indicates a conformation that differs significantly from those of the other peptides but still is partly α-helical (40%).

Contributions from Tryptophan Residues to CD Spectra. Quantification of the secondary structure in proteins and peptides with a large fraction of aromatic residues is generally difficult since these often make significant contributions to the CD signal (for a review, see ref *53*). Studies on protein conformation using site-directed mutagenesis have indicated a large variability in both shape and intensity of the contributions from tryptophan, tyrosine, and phenylalanine residues (*54*−*56*). Important parameters are apparently the position of these residues relative to structural motifs in the proteins, as well as interactions with neighboring groups. In studies of a 17-mer helical model peptide, Chakrabartty et al. assessed the aromatic side-chain contribution to the far-UV CD by substituting an alanine at the N-terminus of the helix with aromatic residues (*57*). They found that the magnitudes of the tyrosine and tryptophan contributions at 222 nm were as large as 5×10^3 and -3×10^3 deg cm^2/dmol per average residue in the 17-mer peptide, respectively. Moreover, they demonstrated the importance of motional restriction for the aromatic CD signal, since insertion of a few flexible glycine residues between the helix and the aromatic residue abolished the induced CD. In the present study, where the conformations of vesicle-associated peptides are examined, the aromatic residues are likely to be motionally restricted as they dip down into the membrane and it is therefore probable that these residues have a significant effect on the resulting CD spectra. It was therefore of interest to acquire CD spectra of the peptides in aqueous solutions with a high content of trifluoroethanol (TFE), providing an environment where the peptides should form α-helices and the motions of the aromatic residues should be less confined. In this solvent, all peptides exhibited CD spectra characteristic of an α-helix, but the shapes of the spectra varied slightly from those acquired for the vesicle-associated peptides (data not shown). Indeed, the difference spectrum obtained for penetratin when subtracting the "TFE spectrum" from the "DOPC/DOPG" spectrum (Figure 2) was very similar in both shape and magnitude to the difference spectrum between the tryptophan-substituted peptide and the parent peptide presented in ref *62*. PenArg and PenLys both gave a similar result, whereas for Pen2W2F, in which the two tryptophans were substituted with phenylalanines, a positive band ranging from 196 to 226 nm was obtained in the difference spectrum (data not shown), in agreement with the positive phenyl CD signal at 222 nm reported by Chakrabartty et al. These results suggest that the CD spectra obtained for the peptides in vesicle dispersions should be corrected for aromatic contributions. If this is done on the basis of the difference spectra obtained here, the helicities of PenArg, penetratin, and PenLys, as calculated from the mean residue ellipticities at 222 nm, are ∼15% lower than indicated above, whereas that of Pen2W2F is ∼5% higher. Nevertheless, it is conceivable that besides the aromatic contribution, the divergence in the spectra of the peptides in the two types of samples has its origin in different backbone conformations.

Influence of Vesicle Aggregation on Peptide Conformation. We have previously shown that when added to DOPG LUVs above a certain peptide-to-lipid ratio, penetratin induces vesicle aggregation followed by spontaneous disaggregation (*14*). Such a process has, to our knowledge, never been observed before. Interestingly, the aggregation/disaggregation process is strongly coupled to a conformational transition of the peptide from α-helix to β-sheet during aggregation and then back to the α-helical conformation during disaggregation. We obtained similar results for DOPC/DOPG (60/40) liposomes with all four peptides studied here, although the threshold peptide-to-lipid ratio is considerably lower for these vesicles (here ∼1:30 compared to ∼1:15 for DOPG, both in phosphate buffer), most probably due to the considerably lower surface charge density. Also, the time required for disaggregation is significantly longer. A repre-

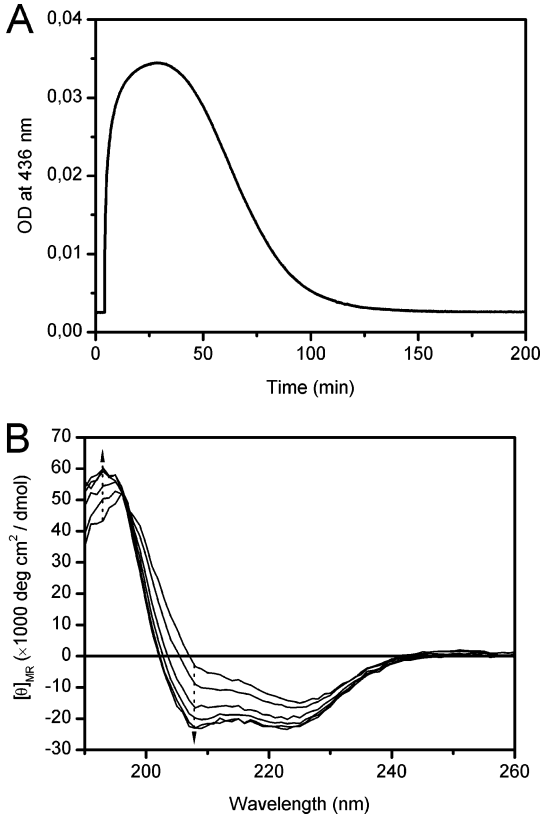

FIGURE 3: Optical density (A) at 436 nm as a function of time with addition of penetratin stock solution (final concentration 0.85 μM) at 4 min to DOPC/DOPG (60/40, 25 μM) vesicles and (B) consecutive circular dichroism spectra collected after penetratin addition (0.85 μM) to a sample containing DOPC/DOPG (60/40, 25 μM) vesicles. Each spectrum is an average of 20 scans recorded during a total of 30 min. The arrows indicate the order of acquisition of the spectra.

sentative illustration of the process is provided in Figure 3, showing changes in optical density (OD) and CD spectrum. After addition of penetratin, six consecutive CD spectra were measured, each spectrum being an average of 20 scans recorded during a total of 30 min. The first spectrum, taken during the first 30 min, deviates significantly from that of an α-helix and is instead indicative of a considerable content of β-structure. The shape of the spectrum is reminiscent of that of an antiparallel β-pleated sheet (*58*), and considering the IR spectroscopy results indicating formation of such penetratin structures in DPPC/DPPS monolayers (*51*), this is assumed to be the structure formed during vesicle aggregation. We are aware that the aggregation is likely to distort the CD spectrum due to effects of light scattering and absorption statistics, the nonzero CD signal between 245 and 260 nm being an indication of this, but there are strong arguments that the CD spectral change on the whole correctly reflects the actual conformational change (see ref *14*). Additional support for this conclusion was provided in titrations of penetratin solution with SDS. When titrating a 0.7 μM penetratin solution with SDS at submicellar concentrations, we obtained a CD spectrum characteristic of an α-helix and not very different from that observed at micellar SDS concentrations (data not shown). The peptide conformation was invariable with SDS concentration between 30 μM and 1 mM except for the concentration range of 60−90 μM SDS. Here, CD spectra similar to those obtained in samples with aggregated vesicles clearly indicated rapid formation

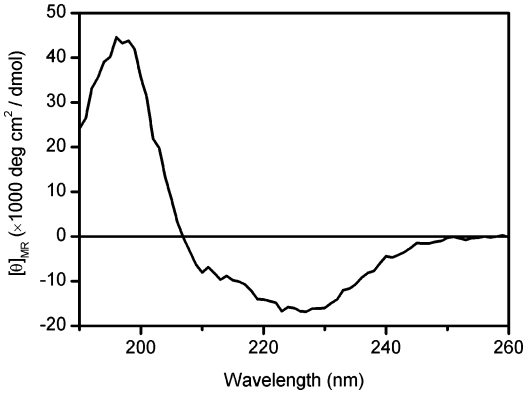

FIGURE 4: Circular dichroism spectrum recorded after addition of penetratin stock solution (final concentration 0.7 μM) to a 75 μM SDS solution. The spectrum is an average of five scans recorded during a total of 7.5 min.

of β-sheets (Figure 4). It is noteworthy that although this process involved a small increase in turbidity, the first few spectra were acquired when the ODs at both 250 and 436 nm were more than an order of magnitude lower than those obtained during peptide-induced aggregation of DOPC/DOPG vesicles (data not shown). The ODs were also lower than in the case of aggregated PEG-PE-containing vesicles, where no contributions of β-sheets could be detected in the CD spectra (see below). When allowed to stand for hours, samples containing β-sheets of penetratin aggregated with SDS exhibited flattening of the CD spectrum, probably due to absorption statistics (*59*), and after even longer time, precipitates could be observed. The α-helix formation, which was obtained for all four peptides at micromolar concentrations of SDS, is consistent with observations of SDS aggregates in the presence of penetratin reported by Berlose et al. (*46*) and suggests that at least under these conditions, SDS molecules are ordered around the peptide. This might, in turn, be taken as a caution to use SDS micelles as models of lipid bilayers. β-sheet formation at submicellar concentrations of SDS has previously been reported for a number of peptides (*60*−*62*) and was also observed for both PenArg and Pen2W2F (data not shown). Interestingly, however, a conformational transition from α-helix to β-sheets could not be obtained with PenLys at any SDS concentration. Although PenLys did form β-sheets during vesicle aggregation, the lack of propensity for β-sheet formation observed here might give a clue to the large differences in cell association observed previously (*10*). In this study, we found that penetratin, PenArg, and Pen2W2F were bound mostly in patches to the plasma membrane and then internalized by the cells, whereas PenLys exhibited almost no cell association.

The penetratin peptides studied here exhibited an α-helix to antiparallel β-sheet transition when going from low to high peptide-to-lipid ratios in vesicle dispersions. A similar behavior has been reported for the Alzheimer β-amyloid peptide (1−40) (*63*), apocytochrome *c* (*64*), and a synthetic peptide (HIV_{Arg}) representing the gp41 N-terminus of LAV_{1a} (*65*). In these three cases, as in ours, β-sheet formation is observed under conditions where aggregation of the liposomes occurs (*64*−*66*). Thus, there seems to be a connection between β-sheet structures and vesicle aggregation. It is, however, difficult to deduce whether aggregation of vesicles induces formation of β-sheets or vice versa, since these

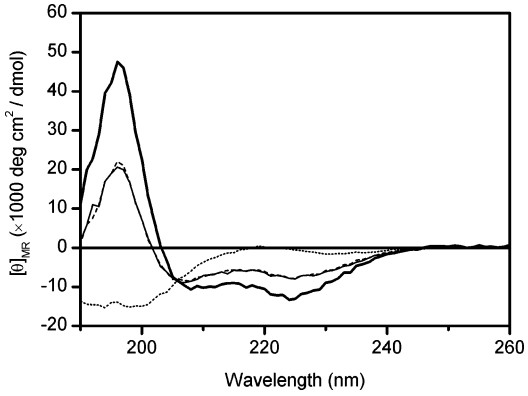

FIGURE 5: Circular dichroism spectra of Pen2W2F bound to DOPC/DOPG/DSPE-PEG(2000) (60/37.5/2.5, 25 μM) liposomes at peptide concentrations of 0.75 μM (thick solid line) and 1.5 μM (thin solid line) and of Pen2W2F (7.5 μM) free in buffer solution (dotted line). The dashed line is the result of a least-squares projection of the spectrum recorded at the high peptide-to-lipid ratio onto the spectrum collected at the low peptide-to-lipid ratio and the free peptide spectrum.

processes are simultaneous. Here, we utilized inclusion of DSPE-PEG(2000) in the liposomes to investigate this issue. Although somewhat less efficient in the phosphate buffer used for CD experiments, the PEG-lipid made it possible to study peptide conformations at peptide-to-lipid ratios much higher than those leading to aggregation of plain DOPC/DOPG (60/40) vesicles. In no case, however, could any β-sheet formation be detected. Even at a peptide-to-lipid ratio of ~1:17, where minor aggregation occurs (the OD at 436 nm increased from ~0.0025 to 0.005−0.007) and a substantial fraction of the peptide is free in solution, the CD spectra obtained could all be perfectly fit to linear combinations of spectra of peptide free in solution and peptide bound to DOPC/DOPG/DSPE-PEG(2000) (60/37.5/2.5) vesicles at low peptide-to-lipid ratios, as shown for Pen2W2F in Figure 5.

Since no formation of β-sheets was observable in any of these experiments, it seems that there exists a threshold peptide-to-lipid ratio for vesicle aggregation but not for β-sheet formation. The implication is that the formation of β-sheets observed is driven by vesicle aggregation. Possibly, the high density of negative charges at the areas of contact in the aggregated vesicles will render the local concentration of peptide in the membrane so high that formation of β-sheets is favored. It could certainly be argued that the PEG chains protruding from the bilayer surface could obstruct β-sheet formation but considering the dimensions of the peptides, these tentacles are rather widely scattered. Moreover, the α-helix to β-sheet transition observed for HIV_{Arg} in POPG LUVs was not affected by the inclusion of 5% DSPE-PEG-(2000) (*27*). The fact that formation of β-sheets was not observed during aggregation of PEG-modified liposomes at exceedingly high peptide-to-lipid ratios could be because the PEG chains, despite vesicle aggregation, may hinder close contact between the adjacent bilayers or because the degree of aggregation is simply too low to generate a significant extent of β-sheet formation. It is also noteworthy that although high peptide concentrations in the membranes of DOPC/DOPG vesicles induce vesicle aggregation, which in turn causes formation of peptide β-structures, the peptides studied here induce only negligible leakage of vesicle-entrapped carboxyfluorescein even at peptide-to-lipid ratios of 1:10 in an induced-leakage assay (data not shown). It thus seems that these processes do not destabilize the vesicle membranes to any greater extent.

CONCLUSIONS

The following has been learned in the present work: (1) The large dissimilarities in cell association previously observed between penetratin, PenArg, and PenLys do not correlate with their corresponding affinities for lipid vesicle membranes but must reflect specific association to other components in the plasma membrane. (2) The inclusion of a small fraction of PEG-conjugated lipids is found to stabilize the vesicles from peptide-induced aggregation and also entails a somewhat increased membrane affinity of the peptides. (3) Vesicle aggregation induced at high peptide-to-lipid ratios drives an α-helix to β-sheet transition, as proven by experiments based on stabilization by PEG-conjugated lipids. (4) For aqueous solutions of penetratin, PenArg, and Pen2W2F, but not for PenLys, an α-helix to β-sheet transition occurs at micromolar concentrations of SDS. (5) The contributions from tryptophan residues to the CD spectra of penetratin analogues are apparently substantially enhanced by the insertion of the chromophore into the lipid bilayer.

ACKNOWLEDGMENT

We thank Christina Brattwall, Petter Isakson, and Åsa Nilsson for help with peptide synthesis.

APPENDIX

Least-Squares Projection Analysis. For construction of binding isotherms, a least-squares projection analysis in combination with singular value decomposition (SVD) was used (*13*, *67*; see also Materials and Methods). The spectra from a titration were collected as columns in a matrix **D**, which was factorized by SVD according to

$$\mathbf{D} = \mathbf{USV}^{\mathrm{T}} \tag{A1}$$

where **U** and **V** have orthonormal columns ($\mathbf{U}^{\mathrm{T}}\mathbf{U} = \mathbf{V}^{\mathrm{T}}\mathbf{V} = \mathbf{I}$) and **S** is zero except along the diagonal, which contains the nonnegative *singular values*. For all peptides, when interacting with both types of vesicles, it was found that only two singular values were significantly larger than zero and that they were the only singular values associated with nonrandom **U** columns. This is consistent with the hypothesis that two species only, free and membrane-bound peptide, account for the emission spectra over the whole titration:

$$\mathbf{D} \approx \mathbf{RC}^{\mathrm{T}} \tag{A2}$$

where **R** is the matrix of reference spectra and **C** is the peptide concentration matrix. **R** thus has two columns, the emission spectra of free and membrane-bound peptide at unit concentration, and the two columns of **C** contain the concentrations of free and membrane-bound peptide, C_f and C_b, in the titration. The concentrations were obtained by a least-squares projection of the emission spectra in **D** on the space of **R**:

$$\mathbf{C}^{\mathrm{T}} = (\mathbf{R}^{\mathrm{T}}\mathbf{R})^{-1}\mathbf{R}^{\mathrm{T}}\mathbf{D} \tag{A3}$$

To ensure a negligible concentration of free peptide during acquistion of the reference spectrum of bound peptide, an excess lipid concentration was used, corresponding to at least 150% of that of the point in the titration where no further blue shift was observed.

Binding Model. The binding model applied in this study was proposed by Beschiaschvili and Seelig (*68*) for binding of cationic peptides to neutral and negatively charged lipid membranes. It is based on the Gouy−Chapman theory in combination with a two-state partition equilibrium and has been employed to describe the membrane association of a number of peptides (*23*, *38*, *41*, *69*, *70*). The surface charge density, σ, of the DOPC/DOPG and DOPC/DOPG/DSPE-PEG(2000) membranes is given by

$$\sigma = (e_0/A_L)\frac{-X_{NL}(1 - X_{Na}) + z_p r}{1 + (A_P/A_L)r} \quad \text{(A4)}$$

where e_0 is the elementary charge, A_L the lateral cross-sectional area per lipid molecule, A_P the effective area of the peptide in the membrane, z_p the effective charge of the peptide, and X_{NL} the mole fraction of negatively charged lipids (DOPG or DSPE-PEG) in the membrane. A_L was assumed to be equal for all three lipids and was set to 70 Å^2. The actual value of A_P for the penetratin peptides has never been measured experimentally. The value (150 Å^2) adopted here and used in our earlier study (*13*) is similar to that used for other peptides (*39*, *41*, *68*), but must be considered rather arbitrarily chosen, since the extent of peptide insertion into the membrane is unknown. However, since r never exceeds 0.065 in our experiments, the contribution from the correction term for peptide insertion, (A_P/A_L)-r, is small compared to unity. The choice of A_P is thus not critical for the calculations. The reduction of the surface charge density due to counterion binding is accounted for by including X_{Na}, which denotes the mole fraction of negatively charged lipids associated with Na^+. It is calculated by assuming a Langmuir adsorption isotherm

$$X_{Na} = \frac{K_{Na}C_{M,Na}}{1 + K_{Na}C_{M,Na}} \quad \text{(A5)}$$

where K_{Na} is the Na^+ binding constant, taken as 0.6 M^{-1} (*71*) for DOPG and assumed to be the same for DSPE-PEG, and $C_{M,Na}$ is the concentration of sodium ions in the close proximity of the membrane surface. $C_{M,Na}$ is connected to the bulk equilibrium concentration, $C_{eq,Na}$, and the surface potential, ψ_0, via a Boltzmann distribution

$$C_{M,Na} = C_{eq,Na}\exp(-\psi_0 F/(RT)) \quad \text{(A6)}$$

where F is the Faraday constant, R the gas constant, and T the absolute temperature.

The surface potential can be determined by combining eq A4 with the Gouy−Chapman equation,

$$\sigma^2 = 2000\epsilon_0\epsilon_r RT\sum_i C_{i,eq}(e^{-z_i F\psi_0/(RT)} - 1) \quad \text{(A7)}$$

where ϵ_0 is the permittivity in a vacuum, ϵ_r denotes the relative dielectric permittivity of water, $C_{i,eq}$ is the bulk concentration of the ith ion, and z_i is its signed valency. The peptide concentration immediately above the membrane surface, C_M, is given by

$$C_M = C_f\exp(-z_p F\psi_0/(RT)) \quad \text{(A8)}$$

Having thus accounted for the electrostatic interaction between the peptide and the membrane, the binding can be described by a surface partition equilibrium

$$r = K_p C_M \quad \text{(A9)}$$

where K_p is the surface partition constant.

For a range of z_p values, equations A4−A8 were solved for each experimental value of r and C_f. The resulting C_M values were plotted against r in search of the z_p that corresponds to the best fit to the experimental data according to eq A9. C_M is always orders of magnitude higher than C_f, reflecting the strong electrostatic attraction between the membrane, with its negative surface potential, and the positively charged peptide.

REFERENCES

1. Lindgren, M., Hällbrink, M., Prochiantz, A., and Langel, Ü. (2000) Cell-penetrating peptides, *Trends Pharmacol. Sci. 21*, 99−103.
2. Wadia, J. S., and Dowdy, S. F. (2002) Protein transduction technology, *Curr. Opin. Biotechnol. 13*, 52−56.
3. Derossi, D., Joliot, A. H., Chassaing, G., and Prochiantz, A. (1994) The third helix of the Antennapedia homeodomain translocates through biological membranes, *J. Biol. Chem. 269*, 10444−10450.
4. Derossi, D., Calvet, S., Trembleau, A., Brunissen, A., Chassaing, G., and Prochiantz, A. (1996) Cell internalization of the third helix of the Antennapedia homeodomain is receptor-independent, *J. Biol. Chem. 271*, 18188−18193.
5. Fischer, P. M., Zhelev, N. Z., Wang, S., Melville, J. E., Fåhraeus, R., and Lane, D. P. (2000) Structure−activity relationship of truncated and substituted analogues of the intracellular delivery vector Penetratin, *J. Pept. Res. 55*, 163−172.
6. Futaki, S., Suzuki, T., Ohashi, W., Yagami, T., Tanaka, S., Ueda, K., and Sugiura, Y. (2001) Arginine-rich peptides. An abundant source of membrane-permeable peptides having potential as carriers for intracellular protein delivery, *J. Biol. Chem. 276*, 5836−5840.
7. Suzuki, T., Futaki, S., Niwa, M., Tanaka, S., Ueda, K., and Sugiura, Y. (2002) Possible existence of common internalization mechanisms among arginine- rich peptides, *J. Biol. Chem. 277*, 2437−2443.
8. Lundberg, M., and Johansson, M. (2002) Positively charged DNA-binding proteins cause apparent cell membrane translocation, *Biochem. Biophys. Res. Commun. 291*, 367−371.
9. Richard, J. P., Melikov, K., Vives, E., Ramos, C., Verbeure, B., Gait, M. J., Chernomordik, L. V., and Lebleu, B. (2003) Cell-penetrating peptides. A reevaluation of the mechanism of cellular uptake, *J. Biol. Chem. 278*, 585−590.
10. Thorén, P. E. G., Persson, D., Isakson, P., Goksör, M., Önfelt, A., and Nordén, B. (2003) Uptake of analogues of penetratin, Tat-(48−60) and oligoarginine in live cells, *Biochem. Biophys. Res. Commun. 307*, 100−107.
11. Lindsay, M. A. (2002) Peptide-mediated cell delivery: application in protein target validation, *Curr. Opin. Pharmacol. 2*, 587−594.
12. Fischer, P. M., Krausz, E., and Lane, D. P. (2001) Cellular delivery of impermeable effector molecules in the form of conjugates with peptides capable of mediating membrane translocation, *Bioconjugate Chem. 12*, 825−841.
13. Persson, D., Thorén, P. E. G., Herner, M., Lincoln, P., and Nordén, B. (2003) Application of a novel analysis to measure the binding of the membrane-translocating peptide penetratin to negatively charged liposomes, *Biochemistry 42*, 421−429.
14. Persson, D., Thorén, P. E. G., and Nordén, B. (2001) Penetratin-induced aggregation and subsequent dissociation of negatively charged phospholipid vesicles, *FEBS Lett. 505*, 307−312.
15. Thorén, P. E. G., Persson, D., Karlsson, M., and Nordén, B. (2000) The Antennapedia peptide penetratin translocates across lipid bilayers − the first direct observation, *FEBS Lett. 482*, 265−268.

16. Mayer, L. D., Hope, M. J., and Cullis, P. R. (1986) Vesicles of variable sizes produced by a rapid extrusion procedure, *Biochim. Biophys. Acta 858*, 161−168.
17. New, R. R. C. (1990) in *Liposomes − a practical approach* (New, R. R. C., Ed.) pp 108−109, IRL Press/Oxford University Press, Oxford, U.K.
18. Gill, S. C., and Vonhippel, P. H. (1989) Calculation of protein extinction coefficients from amino acid sequence data, *Anal. Biochem. 182*, 319−326.
19. Chen, Y. H., Yang, J. T., and Chau, K. H. (1974) Determination of the helix and beta form of proteins in aqueous solution by circular dichroism, *Biochemistry 13*, 3350−3359.
20. Polozov, I. V., Polozova, A. I., Mishra, V. K., Anantharamaiah, G. M., Segrest, J. P., and Epand, R. M. (1998) Studies of kinetics and equilibrium membrane binding of class A and class L model amphipathic peptides, *Biochim. Biophys. Acta-Biomembr. 1368*, 343−354.
21. Chico, D. E., Given, R. L., and Miller, B. T. (2003) Binding of cationic cell-permeable peptides to plastic and glass, *Peptides 24*, 3−9.
22. Seelig, A., and Macdonald, P. M. (1989) Binding of a neuropeptide, substance-P, to neutral and negatively charged lipids, *Biochemistry 28*, 2490−2496.
23. Breukink, E., Ganz, P., de Kruijff, B., and Seelig, J. (2000) Binding of nisin Z to bilayer vesicles as determined with isothermal titration calorimetry, *Biochemistry 39*, 10247−10254.
24. Needham, D., McIntosh, T. J., and Lasic, D. D. (1992) Repulsive interactions and mechanical stability of polymer-grafted lipid membranes, *Biochim. Biophys. Acta 1108*, 40−48.
25. Woodle, M. C., and Lasic, D. D. (1992) Sterically stabilized liposomes, *Biochim. Biophys. Acta 1113*, 171−199.
26. Basanez, G., Goni, F. M., and Alonso, A. (1997) Poly(ethylene glycol)-lipid conjugates inhibit phospholipase C− induced lipid hydrolysis, liposome aggregation and fusion through independent mechanisms, *FEBS Lett. 411*, 281−286.
27. Saez-Cirion, A., and Nieva, J. L. (2002) Conformational transitions of membrane-bound HIV-1 fusion peptide, *Biochim. Biophys. Acta-Biomembr. 1564*, 57−65.
28. Schwarz, G., and Beschiaschvili, G. (1989) Thermodynamic and kinetic studies on the association of melittin with a phospholipid bilayer, *Biochim. Biophys. Acta 979*, 82−90.
29. Stankowski, S. (1991) Surface charging by large multivalent molecules − extending the standard Gouy−Chapman treatment, *Biophys. J. 60*, 341−351.
30. Carnie, S., and McLaughlin, S. (1983) Large divalent cations and electrostatic potentials adjacent to membranes. A theoretical calculation, *Biophys. J. 44*, 325−332.
31. Allen, C., Dos Santos, N., Gallagher, R., Chiu, G. N. C., Shu, Y., Li, W. M., Johnstone, S. A., Janoff, A. S., Mayer, L. D., Webb, M. S., and Bally, M. B. (2002) Controlling the physical behavior and biological performance of liposome formulations through use of surface grafted poly(ethylene glycol), *Biosci. Rep. 22*, 225−250.
32. Vermette, P., and Meagher, L. (2003) Interactions of phospholipid- and poly(ethylene glycol)- modified surfaces with biological systems: relation to physico- chemical properties and mechanisms, *Colloids Surf., B 28*, 153−198.
33. Allende, D., Vidal, A., Simon, S. A., and McIntosh, T. J. (2003) Bilayer interfacial properties modulate the binding of amphipathic peptides, *Chem. Phys. Lipids 122*, 65−76.
34. Rex, S., Bian, J., Silvius, J. R., and Lafleur, M. (2002) The presence of PEG-lipids in liposomes does not reduce melittin binding but decreases melittin-induced leakage, *Biochim. Biophys. Acta-Biomembr. 1558*, 211−221.
35. Nikolova, A. N., and Jones, M. N. (1996) Effect of grafted PEG-2000 on the size and permeability of vesicles, *Biochim. Biophys. Acta-Lipids Lipid Metab. 1304*, 120−128.
36. Nicholas, A. R., Scott, M. J., Kennedy, N. I., and Jones, M. N. (2000) Effect of grafted poly(ethylene glycol) (PEG) on the size, encapsulation efficiency and permeability of vesicles, *Biochim. Biophys. Acta-Biomembr. 1463*, 167−178.
37. Spiwongsitanont, S., and Ueno, M. (2002) Physicochemical properties of PEG-grafted liposomes, *Chem. Pharm. Bull. 50*, 1238−1244.
38. Wieprecht, T., Apostolov, O., Beyermann, M., and Seelig, J. (1999) Thermodynamics of the alpha-helix-coil transition of amphipathic peptides in a membrane environment: Implications for the peptide-membrane binding equilibrium, *J. Mol. Biol. 294*, 785−794.
39. Beschiaschvili, G., and Seelig, J. (1990) Melittin binding to mixed phosphatidylglycerol phosphatidylcholine membranes, *Biochemistry 29*, 52−58.
40. Cantor, C. R., and Schimmel, P. R. (1980) *Biophysical chemistry*, Vol. 1, W. H. Freeman, San Fransisco.
41. Seelig, A., Alt, T., Lotz, S., and Holzemann, G. (1996) Binding of substance P agonists to lipid membranes and to the neurokinin-1 receptor, *Biochemistry 35*, 4365−4374.
42. White, S. H., and Wimley, W. C. (1998) Hydrophobic interactions of peptides with membrane interfaces, *Biochim. Biophys. Acta-Rev. Biomembr. 1376*, 339−352.
43. Ladokhin, A. S., and White, S. H. (1999) Folding of amphipathic alpha-helices on membranes: Energetics of helix formation by melittin, *J. Mol. Biol. 285*, 1363−1369.
44. Wimley, W. C., and White, S. H. (1996) Experimentally determined hydrophobicity scale for proteins at membrane interfaces, *Nat. Struct. Biol. 3*, 842−848.
45. Best, M. D., Tobey, S. L., and Anslyn, E. V. (2003) Abiotic guanidinium containing receptors for anionic species, *Coord. Chem. Rev. 240*, 3−15.
46. Berlose, J. P., Convert, O., Derossi, D., Brunissen, A., and Chassaing, G. (1996) Conformational and associative behaviours of the third helix of antennapedia homeodomain in membrane-mimetic environments, *Eur. J. Biochem. 242*, 372−386.
47. Drin, G., Demene, H., Temsamani, J., and Brasseur, R. (2001) Translocation of the pAntp peptide and its amphipathic analogue AP-2AL, *Biochemistry 40*, 1824−1834.
48. Czajlik, A., Mesko, E., Penke, B., and Perczel, A. (2002) Investigation of penetratin peptides. Part 1. The environment dependent conformational properties of penetratin and two of its derivatives, *J. Pept. Sci. 8*, 151−171.
49. Lindberg, M., and Gräslund, A. (2001) The position of the cell penetrating peptide penetratin in SDS micelles determined by NMR, *FEBS Lett. 497*, 39−44.
50. Magzoub, M., Eriksson, L. E. G., and Gräslund, A. (2002) Conformational states of the cell-penetrating peptide penetratin when interacting with phospholipid vesicles: effects of surface charge and peptide concentration, *Biochim. Biophys. Acta-Biomembr. 1563*, 53−63.
51. Bellet-Amalric, E., Blaudez, D., Desbat, B., Graner, F., Gauthier, F., and Renault, A. (2000) Interaction of the third helix of Antennapedia homeodomain and a phospholipid monolayer, studied by ellipsometry and PM-IRRAS at the air−water interface, *Biochim. Biophys. Acta-Biomembr. 1467*, 131−143.
52. Magzoub, M., Eriksson, L. E. G., and Graslund, A. (2003) Comparison of the interaction, positioning, structure induction and membrane perturbation of cell-penetrating peptides and nontranslocating variants with phospholipid vesicles, *Biophys. Chem. 103*, 271−288.
53. Woody, R. W., and Dunker, A. K. (1996) in *Circular Dichroism and the Conformational Analysis of Biomolecules* (Fasman, G. D., Ed.) pp 109−157, Plenum Press, New York.
54. Andersson, D., Carlsson, U., and Freskgard, P. O. (2001) Contribution of tryptophan residues to the CD spectrum of the extracellular domain of human tissue factor − Application in folding studies and prediction of secondary structure, *Eur. J. Biochem. 268*, 1118−1128.
55. Freskgard, P. O., Martensson, L. G., Jonasson, P., Jonsson, B. H., and Carlsson, U. (1994) Assignment of the contribution of the tryptophan residues to the circular-dichroism spectrum of human carbonic-anhydrase II, *Biochemistry 33*, 14281−14288.
56. Vuilleumier, S., Sancho, J., Loewenthal, R., and Fersht, A. R. (1993) Circular-dichroism studies of barnase and its mutants − characterization of the contribution of aromatic side-chains, *Biochemistry 32*, 10303−10313.
57. Chakrabartty, A., Kortemme, T., Padmanabhan, S., and Baldwin, R. L. (1993) Aromatic side-chain contribution to far-ultraviolet circular- dichroism of helical peptides and its effect on measurement of helix propensities, *Biochemistry 32*, 5560−5565.
58. Perczel, A., Park, K., and Fasman, G. D. (1992) Analysis of the circular-dichroism spectrum of proteins using the convex constraint algorithm − a practical guide, *Anal. Biochem. 203*, 83−93.
59. Duysens, L. N. M. (1956) Flattening of the absorption spectrum of suspensions, as compared to that of solutions, *Biochim. Biophys. Acta 19*, 1−12.
60. Zhong, L. X., and Johnson, W. C. (1992) Environment affects amino acid preference for secondary structure, *Proc. Natl. Acad. Sci. U.S.A. 89*, 4462−4465.

61. Waterhous, D. V., and Johnson, W. C. (1994) Importance of environment in determining secondary structure in proteins, *Biochemistry 33*, 2121−2128.
62. Najbar, L. V., Craik, D. J., Wade, J. D., Salvatore, D., and McLeish, M. J. (1997) Conformational analysis of LYS(11−36), a peptide derived from the beta-sheet region of T4 lysozyme, in TFE and SDS, *Biochemistry 36*, 11525−11533.
63. Terzi, E., Holzemann, G., and Seelig, J. (1997) Interaction of Alzheimer beta-amyloid peptide(1−40) with lipid membranes, *Biochemistry 36*, 14845−14852.
64. Muga, A., Mantsch, H. H., and Surewicz, W. K. (1991) Apocytochrome-C interaction with phospholipid-membranes studied by Fourier transform infrared-spectroscopy, *Biochemistry 30*, 2629−2635.
65. Rafalski, M., Lear, J. D., and Degrado, W. F. (1990) Phospholipid interactions of synthetic peptides representing the N-terminus of Hiv gp41, *Biochemistry 29*, 7917−7922.
66. McLaurin, J., and Chakrabartty, A. (1997) Characterization of the interactions of Alzheimer beta-amyloid peptides with phospholipid membranes, *Eur. J. Biochem. 245*, 355−363.
67. Lawson, C. L., and Hanson, R. J. (1974) *Solving least squares problems*, Prentice-Hall, New Jersey.
68. Beschiaschvili, G., and Seelig, J. (1990) Peptide binding to lipid bilayers − binding isotherms and zeta- potential of a cyclic somatostatin analogue, *Biochemistry 29*, 10995−11000.
69. Seelig, J., Nebel, S., Ganz, P., and Bruns, C. (1993) Electrostatic and nonpolar peptide-membrane interactions − lipid-binding and functional properties of somatostatin analogues of charge $z = +1$ to $z = +3$, *Biochemistry 32*, 9714−9721.
70. Ziegler, A., Li Blatter, X., Seelig, A., and Seelig, J. (2003) Protein transduction domains of HIV-1 and SIV TAT interact with charged lipid vesicles. Binding mechanism and thermodynamic analysis, *Biochemistry 42*, 9185−9194.
71. Eisenberg, M., Gresalfi, T., Riccio, T., and McLaughlin, S. (1979) Adsorption of monovalent cations to bilayer membranes containing negative phospholipids, *Biochemistry 18*, 5213−5223.

BI036054D